NASA/CR–2001–210850

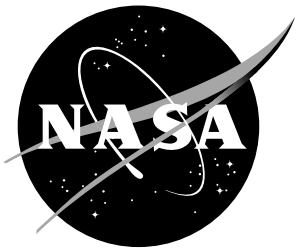

Summary Report of the Orbital X-34 Wing Static Aeroelastic Study

Ramadas K. Prabhu
Lockheed Martin Engineering & Sciences Company, Hampton, Virginia

April 2001

The NASA STI Program Office ... in Profile

Since its founding, NASA has been dedicated to the advancement of aeronautics and space science. The NASA Scientific and Technical Information (STI) Program Office plays a key part in helping NASA maintain this important role.

The NASA STI Program Office is operated by Langley Research Center, the lead center for NASA's scientific and technical information. The NASA STI Program Office provides access to the NASA STI Database, the largest collection of aeronautical and space science STI in the world. The Program Office is also NASA's institutional mechanism for disseminating the results of its research and development activities. These results are published by NASA in the NASA STI Report Series, which includes the following report types:

- TECHNICAL PUBLICATION. Reports of completed research or a major significant phase of research that present the results of NASA programs and include extensive data or theoretical analysis. Includes compilations of significant scientific and technical data and information deemed to be of continuing reference value. NASA counterpart of peer-reviewed formal professional papers, but having less stringent limitations on manuscript length and extent of graphic presentations.

- TECHNICAL MEMORANDUM. Scientific and technical findings that are preliminary or of specialized interest, e.g., quick release reports, working papers, and bibliographies that contain minimal annotation. Does not contain extensive analysis.

- CONTRACTOR REPORT. Scientific and technical findings by NASA-sponsored contractors and grantees.

- CONFERENCE PUBLICATION. Collected papers from scientific and technical conferences, symposia, seminars, or other meetings sponsored or cosponsored by NASA.

- SPECIAL PUBLICATION. Scientific, technical, or historical information from NASA programs, projects, and missions, often concerned with subjects having substantial public interest.

- TECHNICAL TRANSLATION. English-language translations of foreign scientific and technical material pertinent to NASA's mission.

Specialized services that help round out the STI Program Office's diverse offerings include creating custom thesauri, building customized databases, organizing and publishing research results... even providing videos.

For more information about the NASA STI Program Office, see the following:

- Access the NASA STI Program Home Page at ***http://www.sti.nasa.gov***

- E-mail your question via the Internet to help@sti.nasa.gov

- Fax your question to the NASA STI Help Desk at (301) 621–0134

- Phone the NASA STI Help Desk at (301) 621–0390

- Write to:
  NASA STI Help Desk
  NASA Center for AeroSpace Information
  7121 Standard Drive
  Hanover, MD 21076–1320

NASA/CR–2001–210850

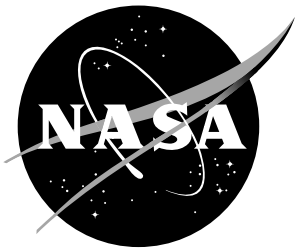

Summary Report of the Orbital X-34 Wing Static Aeroelastic Study

Ramadas K. Prabhu
Lockheed Martin Engineering & Sciences Company, Hampton, Virginia

National Aeronautics and
Space Administration

Langley Research Center
Hampton, Virginia 23681–2199

Prepared for Langley Reseach Center
under contract NAS1-96014

April 2001

Available from the following:

NASA Center for AeroSpace Information (CASI)
7121 Standard Drive
Hanover, MD 21076–1320
(301) 621–0390

National Technical Information Service (NTIS)
5285 Port Royal Road
Springfield, VA 22161–2171
(703) 487–4650

Summary

This report documents the results of a computational study conducted on the Orbital Sciences X-34 configuration. The purpose of this study was to compute the inviscid aerodynamic characteristics of the X-34 wing taking into account its structural flexibility. This was a joint exercise conducted with Structural Dynamics Research Corporation (SDRC) of California, who provided the wing structural deformations for a given pressure distribution on the wing surfaces. This study was done for a Mach number of 1.35 and an angle of attack of 9 deg.; the freestream dynamic pressure was assumed to be 607 lb/ft^2. Only the wing and the body were simulated. Two wing configurations were examined. The first had the elevons in the undeflected position and the second had the elevons deflected 20 degrees up. The results indicated that with undeflected elevons, the wing twists by about 1.5 deg. resulting in a reduction in the angle of attack at the wing tip by 1.5 deg. The maximum vertical deflection of the wing is about 3.71 inches at the wing tip. For the wing with the undeflected elevons, the effect of this wing deformation is to reduce the normal force coefficient (C_N) by 0.012 and introduce a nose up pitching moment coefficient (C_m) of 0.042. With the elevons deflected 20 degrees up, the effects are relatively small. The C_N increases by 0.003 and the C_m decreases by 0.013.

Nomenclature

C_A	$\mathbf{F_x}/(q_\infty\ S_{ref})$, Axial force coefficient
C_N	$\mathbf{F_z}/(q_\infty\ S_{ref})$, Normal force coefficient
C_m	$\mathbf{M_y}/(q_\infty\ S_{ref}\ l_{ref})$, Pitching moment coefficient
C_p	$(p - p_\infty)/q_\infty$, Pressure coefficient
$\mathbf{F_x}$	Axial force, (lb)
$\mathbf{F_y}$	Side force, (lb)
$\mathbf{F_z}$	Normal force, (lb)
l_{ref}	Reference length (=174.48 in.)
$\mathbf{M_x}$	Rolling moment, (ft.lb)
$\mathbf{M_y}$	Pitching moment, (ft.lb)
$\mathbf{M_z}$	Yawing moment, (ft.lb)
	NOTE: The moment reference point is at (0, 0, 0).
M_∞	Freestream Mach number (=1.35)
p	Static pressure on the wing surface
p_∞	Freestream static pressure
q_∞	Freestream dynamic pressure (=607 lb/ft^2)
S_{ref}	Reference area (=51480.0 sq. in.)
x, y, z	Cartesian co-ordinates of a given point; (The nose is at 92.62in., 0, -23.62in.) (The x-axis is in the axial direction, the y-axis is in the spanwise direction, and the z-axis is in the vertical direction)
α	Angle of attack, deg.
Δx, Δy, Δz	Displacements of a point along the x, y, and z axes, respectively, (in.)

Figure 1: A Sketch of the X-34 model used for the wing static aeroelastic studies.

Introduction

The purpose of this study was to determine the effect of the X-34 wing structural flexibility on the static longitudinal aerodynamic characteristics. In this study only the wing was assumed to be flexible, and all other components of the vehicle were assumed to be rigid. Due to the spanwise load distribution the wing is deflected and due to the chordwise distribution the wing is twisted. Since the wing twist changes the angle of attack along the wing span, it has a much larger impact on the wing aerodynamic characteristics than the wing bending. In the present study, the effect of the wing flexibility on its aerodynamic characteristics are computed iteratively.

Under a contractual agreement with Orbital Sciences, SDRC of San Diego modeled the structural details of the wing. Surface pressures on the Outer Mold Line (OML) were computed at LaRC and transmitted to SDRC. SDRC then transferred the loads to the underlying wing structure, and computed the wing structural deflections. The deflected wing geometry was then returned to LaRC for further computational analysis.

The major components of the X-34 vehicle are the fuselage, the wing, the bodyflap, the engine bell, and the rudder. Of these, the bodyflap, the engine bell, and the rudder are located sufficiently far behind the wing trailing edge to preclude any upstream influence on the wing at Mach 1.35. Since the purpose of the study was to determine the pressure distribution on the wing and compute its aerodynamic characteristics, it was decided to simplify the computational model by simulating only the wing and the body in the CFD model and deleting the bodyflap, the engine bell, and the rudder. Since the vehicle has a plane of symmetry, only one half of the vehicle was modeled. The CFD model has a wing semispan of 166.30 in. and a length of 646.88 in. A sketch of the CFD model is shown Fig. 1.

The present studies were conducted for a freestream Mach number of 1.35 and an angle of attack of 9 degrees. The freestream dynamic pressure was 607 lb/ft^2 which represents the maximum dynamic pressure on a reference trajectory. Two wing configurations were studied; the first was with the elevons undeflected, and the second was with the elevons deflected 20 deg. up.

The FELISA Software

All the computations of the present study were done using the FELISA unstructured grid software. This software package consists of a set of computer codes for the simulation of three dimensional steady inviscid flows using unstructured tetrahedral element grids. Surface triangulation and discretization of the computational domain using tetrahedral elements is done by two separate codes. There are two inviscid flow solvers—one for transonic flows and the other for hypersonic flows with an option for perfect gas air, equilibrium air, and CF_4 gases. The transonic flow solver was used for the present study. The ratio of specific heats, (γ), was assumed to be 1.4. Post-processors like the aerodynamic analysis routine used in the study, are part of the FELISA software package. More information on FELISA may be found in [1].

Computers Used

The surface and volume grid generation as well as pre-processing of the grids and post-processing of the solution was done on an SGI ONYX computer located in the Aerothermodynamics Branch (AB), NASA Langley Research Center. After the FELISA data files were set-up, each surface grid generation required about 30 minutes and each volume grid generation required 4 to 5 CPU hours on the ONYX. Most of the flow computations were done on SGI origin 2000 series parallel processing computers, each having 64 processors sitting on top of 16G of shared memory. Each computation of the flow solution required 32 to 40 CPU hours on these parallel machines.

The X-34 Geometry and the Grids

The geometrical information of the X-34 was received in the form of an IGES file with 67 trimmed surfaces. Of these 29 defined the body and the remaining 38 surfaces defined the wing and elevons. The IGES file was processed using the software GridTool [2], and a set of FELISA data files was obtained. The computational domain was chosen such that the flow would be contained within this domain except at the outflow boundary. A sketch of the computational domain is shown in Fig. 2.

The FELISA data files were manually modified so that the desired grid spacings could be obtained. The grid spacings were chosen such that on and around the wing the spacings were small. Typically, near the wing leading edge the grid spacing was 0.75 inch at the tip and 1.0 inch near the root. In the far field where the flow is not influenced by the vehicle, the grid spacing was large. The FELISA surface grid generator was used to triangulate the surfaces. A typical surface grid used for the present computations is shown in Fig. 3.

After a satisfactory surface grid was obtained, the FELISA volume grid generator was used to generate an unstructured grid of tetrahedral elements within the computational domain. A typical grid used for the present study had about 80,000 points on the surface, and about 650,000 points in the volume grids. All the grids required for this study were generated on the SGI computer at the Aerothermodynamics Branch.

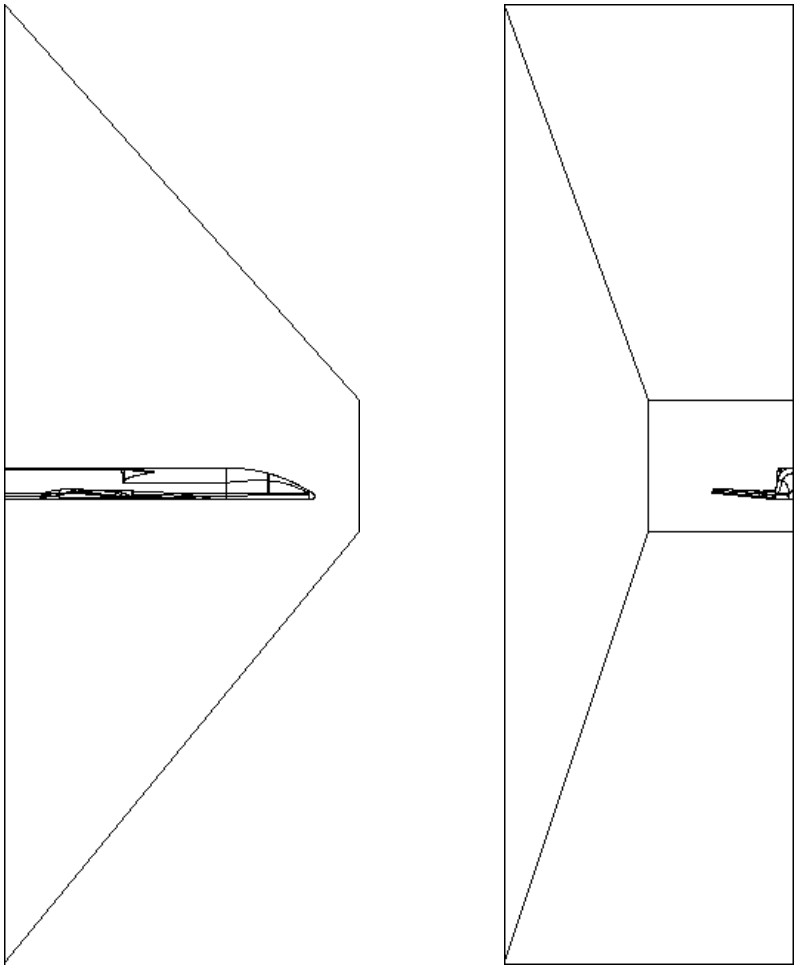

(a) Side view (b) Front view

Figure 2: Computational domain used for X-34 wing static aeroelastic studies.

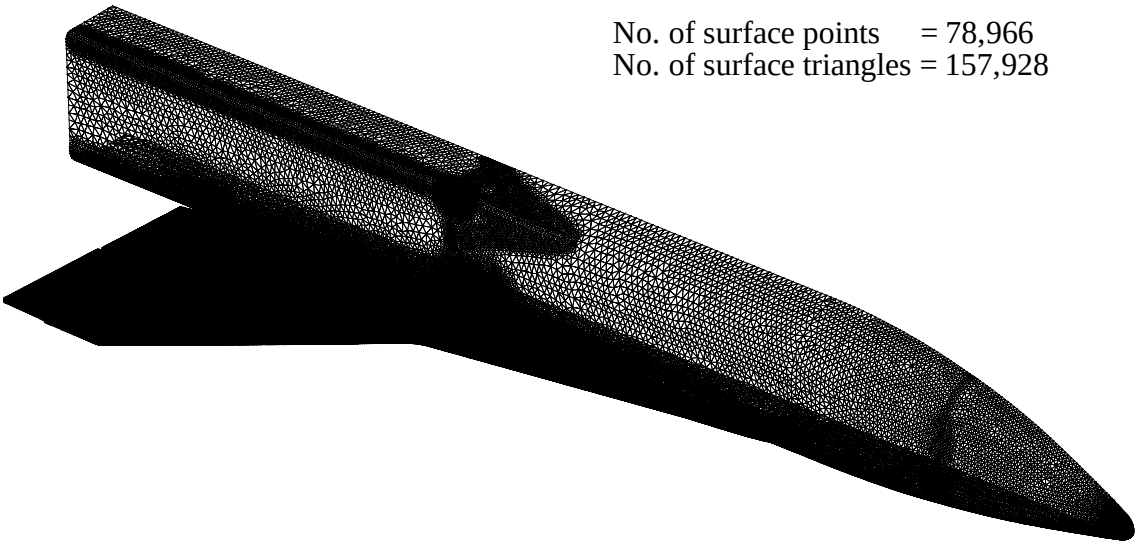

Figure 3: A typical surface triangulation used for the X-34 wing static aeroelastic studies.

Flow Solution

The volume grids were partitioned using the FELISA pre-processor to run on a total of 8 processors. The flow solutions were started with the low-order option and run for a few hundred iteration, and then the higher-order option was turned on. The pressure distribution on the wing and the body was integrated, and the normal force, axial force, and pitching moment were computed once every 20 iteration steps. The solution was assumed to have converged when these loads reached steady values. This normally required a total of 32 to 40 CPU hours.

The solution was post-processed on the SGI ONYX at the AB. The aerodynamic loads acting on the wing were computed, and the pressure distribution on the wing surfaces were extracted. This information was sent to SDRC along with the surface definition of the wing, and additional information on the curves that were common between the wing and the fuselage. Since the fuselage was assumed to be rigid, these curves were constrained and not allowed to undergo any deformation although they were part of the wing. The deformation of the wing due to the prescribed pressure loads was computed by SDRC, and the deformed wing surface geometry was returned to LaRC. This geometry was combined with the data files, and a new set of FELISA data files was obtained for the deformed wing after the first iteration cycle. These data files were then used to generate surface and volume grids for the second iteration cycle.

This process of computing the pressure distribution and a deformed wing shape for the computed pressure distribution was repeated four times. The loads computed on the vehicle at the fourth iteration cycle were practically same as the loads computed in the previous cycle. At this point the process was assumed to have converged.

Results and Discussion

The X-34 structure lies under a layer of TPS material. Therefore the pressure loads computed on the external surfaces (OML) of the vehicle had to be transferred to the structure. Due to the inaccuracies in this load transfer process there were some differences between the aerodynamics loads (resulting from the integration of the computed surface pressure distribution) and the actual loads applied to the structure at each iteration steps. The applied loads deflect the wing structure. Since the deflected wing surface (OML) was required for flow computations, the wing structural deflections had to be transferred back to the wing surface. This step also introduced some inaccuracies.

It should be recalled that the reference point for all the moments is (0, 0, 0). Also, note that the nose of the vehicle is at (92.82in., 0, -26.32in.). The dynamic pressure is assumed to be 607 lb/ft^2.

Case 1: Elevons Undeflected

The computed aerodynamic loads for the undeflected elevons case are summarized in the Table 1.

The actual loads applied to the structure are listed in Table 2. A comparison of Tables 1 and 2 reveals that the difference in the maximum force namely $\mathbf{F_z}$, is about 0.5%, and in the difference in the maximum moment namely $\mathbf{M_y}$, was about 0.4%. These small differences are not expected to significantly affect the findings of the present study.

The undeformed wing tip shape and the deformed shapes are shown in Fig. 4. It may be noticed form this figure that there is little difference between the tip shapes for the third and the fourth iterations. This is an indication that the process has converged. Similar conclusion may be drawn from Fig. 5 where the lines common between the wing and the elevons are plotted. The deflections of the leading and trailing edges at

Iteration No.	Mesh ID	F_x (lb)	F_y (lb)	F_z (lb)	M_x (ft.lb)	M_y (ft.lb)	M_z (ft.lb)
1	X34C11	2949	-16916	48740	309130	-2325000	-741930
2	X34C12	2384	-17393	45876	283460	-2178600	-760330
3	X34C13	2438	-17374	46192	286360	-2194900	-759990
4	X34C14	2426	-17377	46133	285770	-2191800	-760010

Table 1: Computed aerodynamic loads on the X-34 wing, M=1.35, $\alpha = 9$ deg., elevons zero deg.

Iteration No.	F_x (lb)	F_y (lb)	F_z (lb)	M_x (ft.lb)	M_y (ft.lb)	M_z (ft.lb)
1	2311	-16249	48649	307086	-2315754	-702880
2	2249	-16063	46055	284816	-2184652	-692645
3	2261	-16084	46366	287638	-2200593	-693909

Table 2: Loads applied to the X-34 wing structure, M=1.35, $\alpha = 9$ deg., elevons zero deg.

the wing tip for the four iterations are shown in Table 3. It may be noted from this table that the vertical deflection at the trailing edge of the wing tip is 3.71 in. At the leading edge the deflection is 2.09 in. This amounts to a wing twist of about 1.5 deg.

The upper surface C_p contours for the undeformed wing and the wing after the fourth iteration are shown in Fig. 6. It may be observed from this figure that there are small differences between the two contour plots.

The aerodynamic coefficients for the loads shown in Table 1 are listed in Table 4. Note that the reference area and the pitching moment reference length are 51480.0 sq. in. and 174.48 in., respectively, and the pitching moment reference point is the nose of the vehicle. The changes in C_N and C_m due to the wing deformation are -0.012 and +0.042, respectively.

Iteration No.	Leading Edge			Trailing Edge		
	Δx	Δy	Δz	Δx	Δy	Δz
1	0.00	0.00	0.00	0.00	0.00	0.00
2	0.13	-0.19	2.24	0.14	-0.38	4.04
3	0.14	-0.17	2.07	0.13	-0.34	3.65
4	0.14	-0.17	2.09	0.13	-0.35	3.71

Table 3: Deflections the leading and trailing edges at the wing tip, M=1.35, $\alpha = 9$ deg., elevons zero deg.

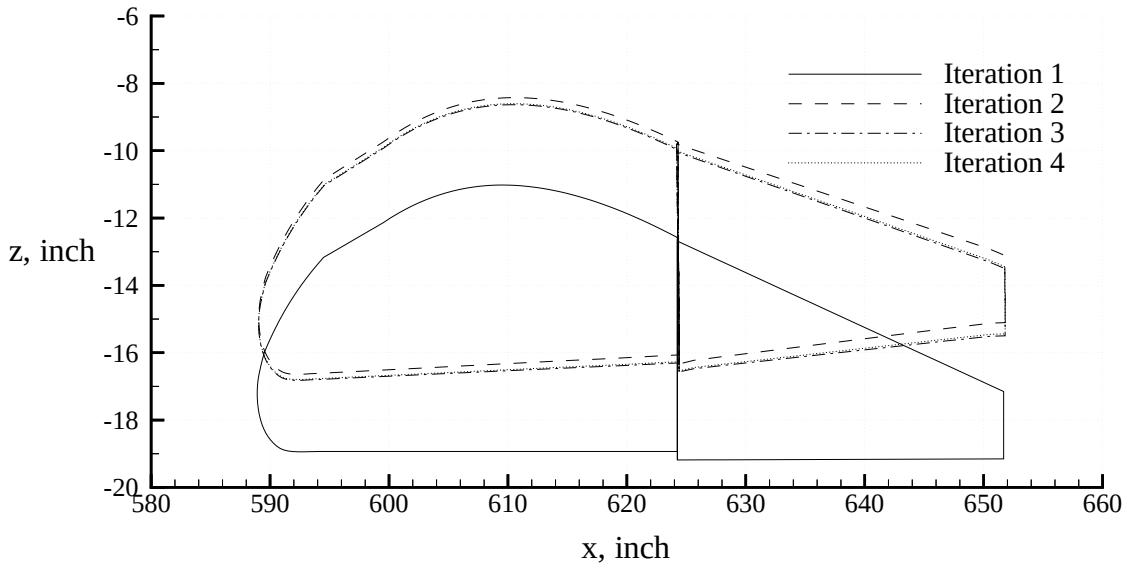

Figure 4: The wing tip section, M=1.35, $\alpha = 9$ deg., elevons zero deg.

Iteration No.	**Mesh ID**	C_A	C_N	C_m
1	X34C11	0.0136	0.2246	-0.7369
2	X34C12	0.0101	0.2114	-0.6905
3	X34C13	0.0112	0.2129	-0.6956
4	X34C14	0.0112	0.2126	-0.6947

Table 4: Computed aerodynamic coefficients for the X-34 Wing, M=1.35 $\alpha = 9$ deg., elevons zero deg.

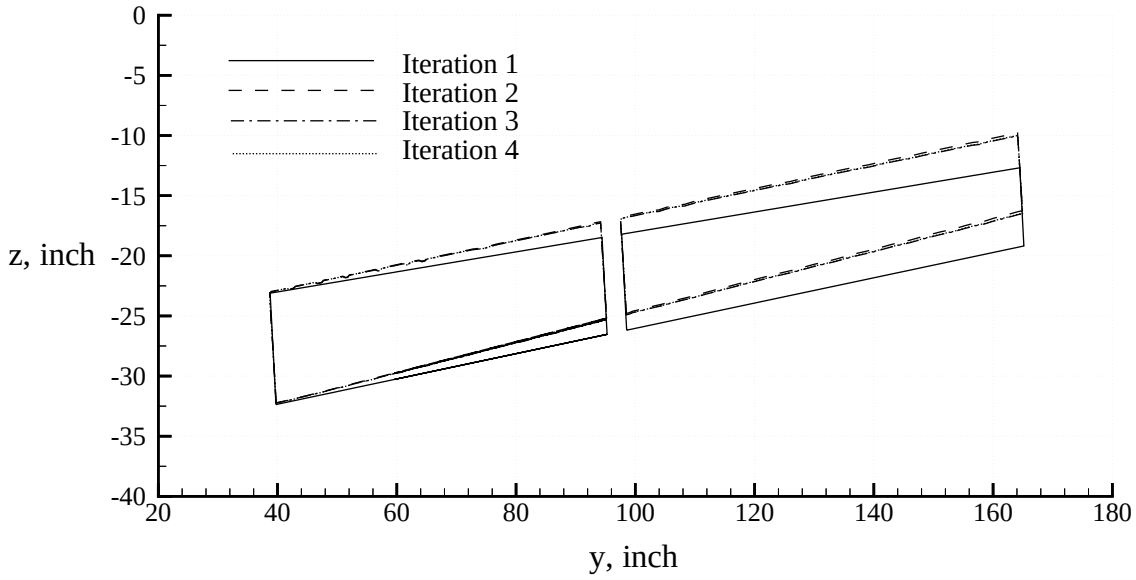

Figure 5: A plot of the wing/elevons common lines, M=1.35, α = 9 deg., elevons zero deg.

Case 2: Elevons Deflected 20 Deg. Up

The computed aerodynamic loads for the case with the elevons deflected 20 deg. up are shown in Table 5. For the reasons noted earlier, there were small differences between the aerodynamics loads (resulting from the computed surface pressure distribution) and the actual loads applied to the structure at these iteration steps is listed in Table 6. It may be noted that the difference in the maximum force namely Fz, was about 0.5difference in the maximum moment namely My, was about 0.4had been noticed in the first case. These small differences are not expected to significantly affect the findings of the present study.

The undeformed and deformed wing tip shapes are shown in Fig. 7. It may be noticed form this figure that there is little difference between the tip shapes for the third and the fourth iterations. This is an indication that the process has converged. Similar conclusion may be drawn from Fig. 8 where the lines common between the wing and the elevons are plotted. The deflections of the leading and trailing edges at the wing tip for the four iterations are shown in Table 7. It may be noted from this table that the maximum vertical deflection of 1.24 in. occurs at the leading edge. This is much smaller compared to the 3.71 in. deflection for the undeflected elevons case.

The C_p contours on the upper surface of the wing before and after deformation are shown in Fig. 9. It may be observed that the differences between these plots are small. The aerodynamic coefficients for the axial and normal forces, and the pitching moment in Table 5 are listed in Table 8. The changes in C_N and C_m due to the wing deformation are +0.003 and -0.013, respectively. These changes are much smaller than in the elevons undeflected case.

It should be recalled at this points that the present computations are inviscid. Hence, the skin friction

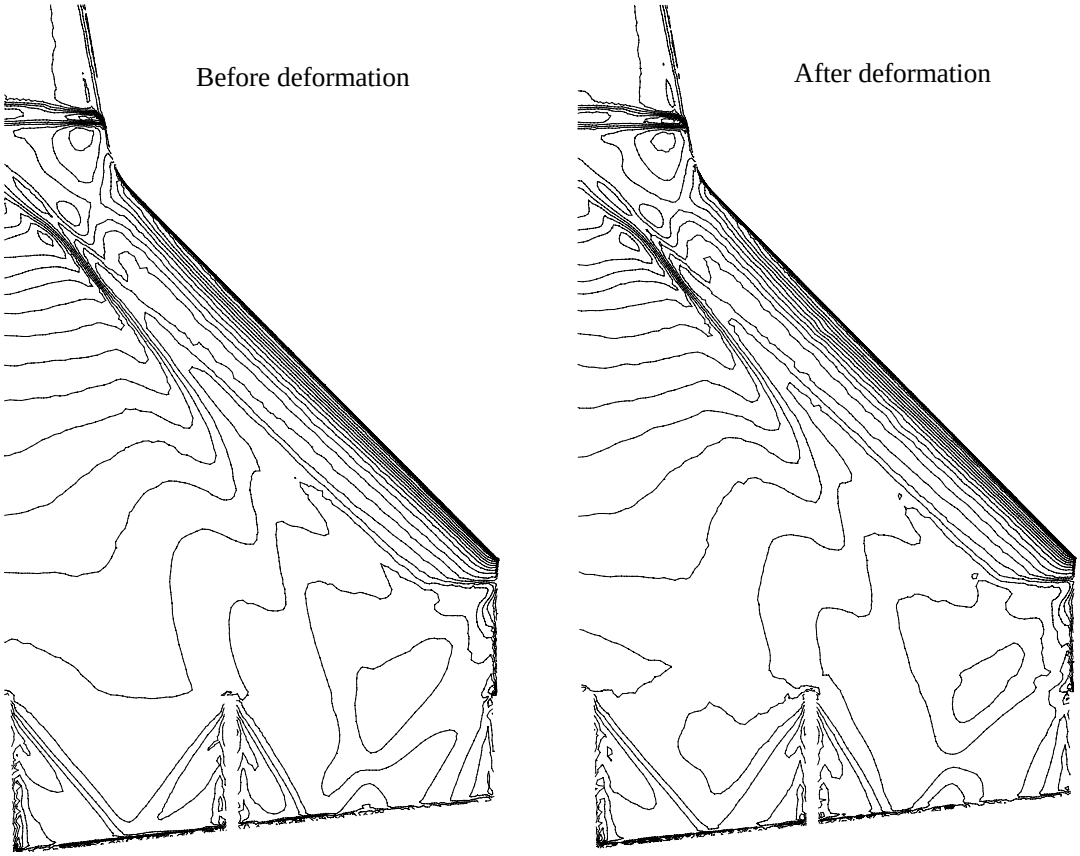

Figure 6: Wing upper surface C_p distribution before and after the wing deformation, M=1.35, α = 9 deg., elevons zero deg.

Iteration No.	**Mesh** ID	$\mathbf{F_x}$ (lb)	$\mathbf{F_y}$ (lb)	$\mathbf{F_z}$ (lb)	$\mathbf{M_x}$ (ft.lb)	$\mathbf{M_y}$ (ft.lb)	$\mathbf{M_z}$ (ft.lb)
1	X34E11	3868	-15432	31904	176380	-1427000	-669040
2	X34E12	3635	-15731	32797	182990	-1475500	-681850
3	X34E13	3644	-15723	32585	181060	-1464600	-681410
4	X34E14	3663	-15742	32638	181540	-1467300	-682590

Table 5: Computed aerodynamic loads on the X-34 wing, M=1.35, α = 9 deg., elevons 20 deg. up.

Iteration No.	F_x (lb)	F_y (lb)	F_z (lb)	M_x (ft.lb)	M_y (ft.lb)	M_z (ft.lb)
1	3193	-14660	31351	171119	-1393538	-624152
2	3040	-14759	32325	178731	-1446474	-628148
3	3063	-14735	32103	176819	-1435192	-627136
4	3050	-14766	32163	177278	-1438054	-628567

Table 6: Loads applied to the X-34 wing structure, M=1.35, $\alpha = 9$ deg., elevons 20 deg. up.

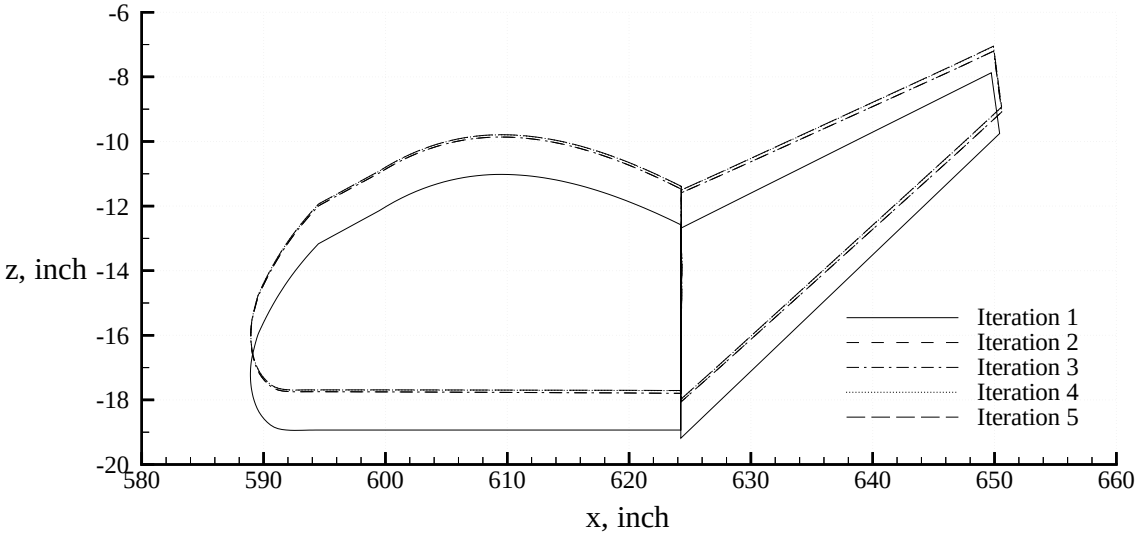

Figure 7: The wing tip section for M=1.35, $\alpha = 9$ deg., elevons 20 deg. up.

Iteration No.	Leading Edge			Trailing Edge		
	Δx	Δy	Δz	Δx	Δy	Δz
1	0.00	0.00	0.00	0.00	0.00	0.00
2	0.03	-0.09	-1.19	0.17	-0.14	-0.66
3	0.04	-0.09	-1.26	0.16	-0.17	-0.84
3	0.04	-0.09	-1.24	0.16	-0.16	-0.81

Table 7: Deflections of the leading and trailing edges at the wing tip, M=1.35, $\alpha = 9$ deg., elevons 20 deg. up.

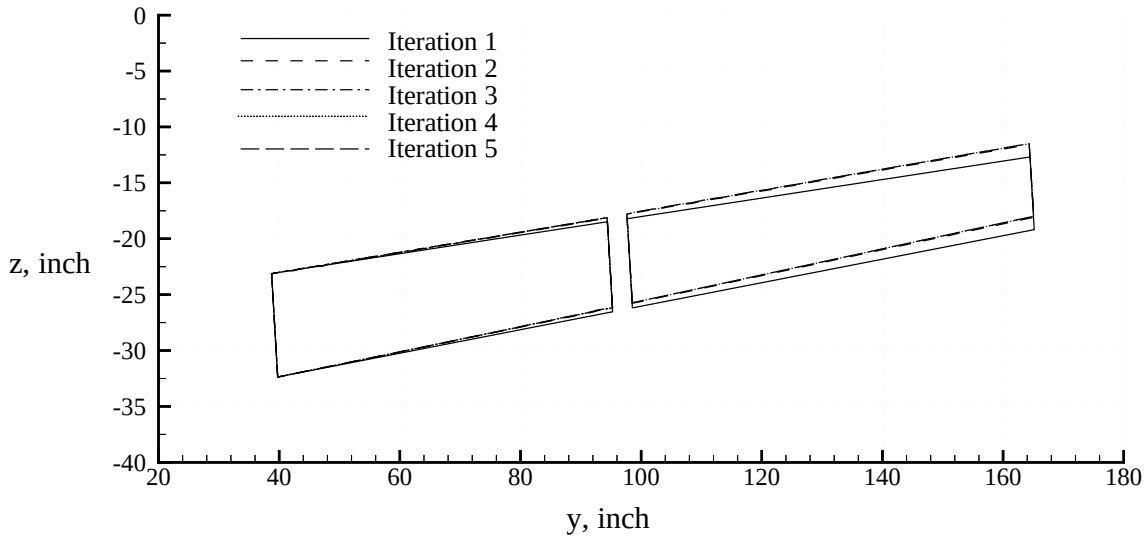

Figure 8: A plot of the wing/elevons common lines for M=1.35, $\alpha = 9$ deg., elevons 20 deg. up.

is absent. This leads to smaller axial force. More importantly, the flow separation, if any, and its effect on the aerodynamic loads is also absent. However, at an angle of attack of 9 deg. for the undeflected elevons case, there would not be significant separation on the wing. With the elevons deflected 20 deg. up, there is a likelihood of flow separation ahead of the elevons hinge line because of a sudden change in slope of the wing surface ahead of the hinge line. Its effect on the findings is not known.

Conclusion

An inviscid computational study was done to determine the effect of the structural flexibility of the X-34 wing on its longitudinal aerodynamic characteristics. The unstructured flow solver FELISA software was used for the grid generation and flow solution. Two wing configurations—one with the elevons in the undeflected

Iteration No.	**Mesh ID**	C_A	C_N	C_m
1	X34E11	0.0178	0.1470	-0.4523
2	X34E12	0.0168	0.1511	-0.4676
3	X34E13	0.0168	0.1502	-0.4642
4	X34E14	0.0169	0.1504	-0.4651

Table 8: Computed aerodynamic coefficients for the X-34 wing, M=1.35, $\alpha = 9$ deg., elevons 20 deg. up.

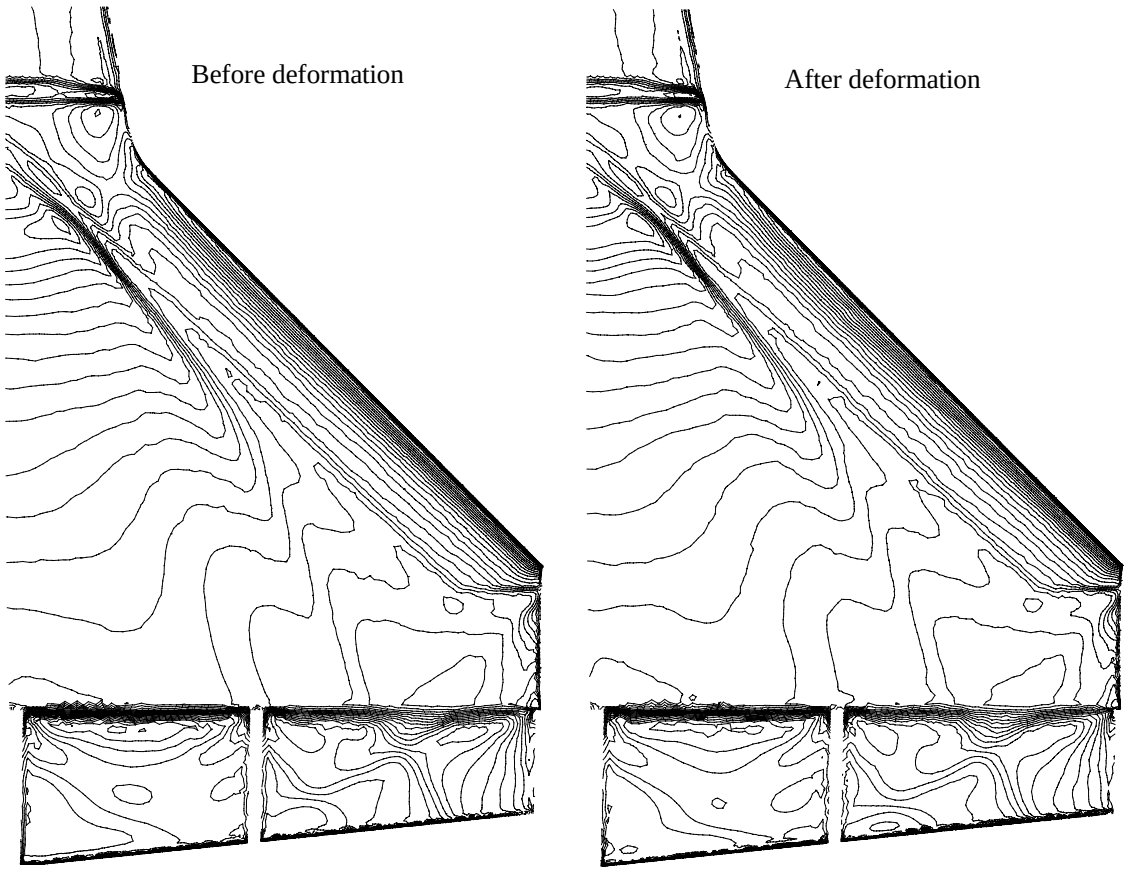

Figure 9: Wing upper surface C_p distribution before and after the wing deformation, M=1.35, α = 9 deg., elevons 20 deg. up.

position and the other with the elevons deflected up 20 deg. were considered. For the wing with undeflected elevons the effect of the wing flexibility was to reduce C_N by 0.012 and change C_m by 0.042 (nose up). For the wing with the elevons deflected 20 deg. up, the effect was to increase the C_N by 0.003, and change the C_m by -0.013 (nose down). The present flow computations are inviscid. Hence, the absence of boundary layer and skin friction could affect the aerodynamic loads and the findings of the present study.

Acknowledgments

The author wishes to express his gratitude to Ms. K. L. Bibb, Mr. K. J. Weilmuenster, and Dr. K. Sutton of the Aerothermodynamics Branch for many helpful discussions during the course of this work. Much of the preliminary work for the static aeroelasticity study was done by Ms. Bibb. The work described herein was performed at Lockheed Martin Engineering & Sciences Company in Hampton, Virginia, and was supported by the Aerothermodynamics Branch, NASA Langley Research Center under the contract NAS1-96014. The technical monitor was K. J. Weilmuenster.

References

[1] Peiro, J., Peraire, J., and Morgan, K., "FELISA System Reference Manual and User's Guide," Tech. Report, University College of Swansea, Swansea, U.K., 1993.

[2] Samereh, J., "GridTool: A Surface Modeling and Grid Generation Tool," NASA CP 3291, May 1995.

REPORT DOCUMENTATION PAGE

Form Approved
OMB No. 0704–0188

1. AGENCY USE ONLY *(Leave blank)*	2. REPORT DATE	3. REPORT TYPE AND DATES COVERED
	April 2001	Contractor Report

4. TITLE AND SUBTITLE
Summary Report of the Orbital X-34 Wing Static Aeroelastic Study

5. FUNDING NUMBERS
C NAS1-96014
WU 242-80-01-01

6. AUTHOR(S)
Ramadas K. Prabhu

7. PERFORMING ORGANIZATION NAME(S) AND ADDRESS(ES)
Lockheed Martin Engineering & Sciences Company
C/O NASA Langley Research Center
Hampton, VA 23681–2199

8. PERFORMING ORGANIZATION REPORT NUMBER

9. SPONSORING/MONITORING AGENCY NAME(S) AND ADDRESS(ES)
NASA Langley Research Center
Hampton, VA 23681–2199

10. SPONSORING/MONITORING AGENCY REPORT NUMBER
NASA/CR–2001–210850

11. SUPPLEMENTARY NOTES
Langley Technical Monitor: K. James Weilmuenster

12a. DISTRIBUTION/AVAILABILITY STATEMENT
Unclassified-Unlimited
Subject Category 02
Distribution: Nonstandard
Availability: NASA CASI (301) 621–0390

12b. DISTRIBUTION CODE

13. ABSTRACT ***(Maximum 200 words)***

This report documents the results of a computational study conducted on the Orbital Sciences X-34 vehicle to compute its inviscid aerodynamic characteristics taking into account the wing structural flexibility. This was a joint exercise between LaRC and SDRC of California. SDRC modeled the structural details of the wing, and provided the structural deformation for a given pressure distribution on its surfaces. This study was done for a Mach number of 1.35 and an angle of attack of 9 deg.; the freestream dynamic pressure was assumed to be 607 lb/ft^2. Only the wing and the body were simulated in the CFD computations. Two wing configurations were examined. The first had the elevons in the undeflected position and the second had the elevons deflected 20 deg. up. The results indicated that with elevon undeflected, the wing twists by about 1.5 deg. resulting in a reduction in the angle of attack at the wing tip to by 1.5 deg. The maximum vertical deflection of the wing is about 3.71 inches at the wing tip. For the wing with the undeflected elevons, the effect of this wing deformation is to reduce the normal force coefficient (C_N) by 0.012 and introduce a nose up pitching moment coefficient (C_m) of 0.042.

14. SUBJECT TERMS
Unstructured grid, CFD, Wing structural flexibility, Aerodynamic loads

15. NUMBER OF PAGES
19

16. PRICE CODE
A03

17. SECURITY CLASSIFICATION OF REPORT	18. SECURITY CLASSIFICATION OF THIS PAGE	19. SECURITY CLASSIFICATION OF ABSTRACT	20. LIMITATION OF ABSTRACT
Unclassified	Unclassified	Unclassified	UL